JOURNAL OF NATURAL PRODUCTS

Article

Cite This: J. Nat. Prod. 2019, 82, 1820−1830

pubs.acs.org/jnp

Molecular Networking Reveals the Chemical Diversity of Selaginellin Derivatives, Natural Phosphodiesterase-4 Inhibitors from *Selaginella tamariscina*

Sunmin Woo,[†] Kyo Bin Kang,[*,‡] Jinwoong Kim,[*,†] and Sang Hyun Sung[†,§]

[†]College of Pharmacy and Research Institute of Pharmaceutical Sciences, Seoul National University, Seoul 08826, Republic of Korea

[‡]Research Institute of Pharmaceutical Sciences, College of Pharmacy, Sookmyung Women's University, Seoul 04310, Republic of Korea

Supporting Information

ABSTRACT: Selaginellins are unique pigments found in the genus *Selaginella*, the largest genus of Lycopodiophyta. Recent studies reported that some selaginellin analogues have potent phosphodiesterase-4 (PDE4) inhibitory activity. In this study, the chemical diversity of natural selaginellin derivatives was revealed by an MS/MS molecular networking-based dereplication of the *Selaginella tamariscina* extract. It led to the prioritization of chromatographic peaks predicted as previously unknown selaginellin derivatives. Targeted isolation of these compounds afforded two unusual selaginellin analogues with a 1*H*,3*H*-dibenzo[*de*,*h*]isochromene skeleton, namely, selariscins A (**1**) and B (**2**), along with eight new diarylfluorene derivatives, selaginpulvilins M−T (**3**−**10**), and five known analogues, **11**−**15**. The absolute configurations of **1**, **2**, and **8**−**10** were elucidated by spectroscopic data analyses including computational electronic circular dichroism data. Compounds **1** and **3**−**10** showed PDE4 inhibitory activity with IC_{50} values in the range of 2.8−33.8 μM, and their binding modes are suggested by a molecular docking study.

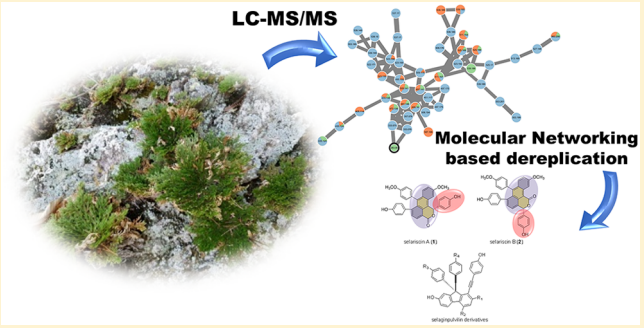

Phosphodiesterase-4 (PDE4) is an important pharmacological target for inflammatory diseases and tumors. PDE4 inhibitors have been pursued for the treatment of diseases such as chronic obstructive pulmonary disease (COPD), rheumatoid arthritis, and various cancers.[1−3] Recently, naturally occurring PDE4 inhibitors have been reported from different species of plants or fungi.[4,5] The genus *Selaginella*, the largest genus of Lycopodiophyta containing about 700 species, is known for its unusual pigment metabolites named selaginellins.[6] Recently, selaginellin analogues were reported to exhibit potent PDE4 inhibitory activity. Fluorene derivatives from *S. pulvinata*, selaginpulvilins A−L, and a 1*H*-2-benzopyran derivative from *S. tamariscina*, selagintamarlin A, exhibited exceptionally potent inhibitory activity against PDE4.[7−10] Inspired by the unprecedented structures and potent bioactivity, the organic chemistry community developed several synthetic methods for selaginpuvilins C and D,[11−13] which shows that selaginellin analogues are promising leads for drug discovery. Despite this important biological activity, the chemical diversity of natural selaginellin derivatives has not been systematically analyzed.

In the present study, we expand our understanding of the chemical diversity of natural PDE4 inhibitory selaginellin derivatives by a structure-based discovery approach with liquid chromatography combined with tandem mass spectrometry (LC−MS/MS) analysis.[14] LC−MS/MS is the most commonly used platform for holistic profiling of natural products, because it provides useful information for structural characterization in complex mixtures.[15,16] There have been a few studies on the chemical profiling of *Selaginella* extracts, but these only characterized primary metabolites or biflavonoids, not the selaginellin derivatives.[17,18] In the current study, we applied an MS/MS molecular networking (MN) strategy,[19] which has been demonstrated as a promising tool for dereplication and structure-based discovery of natural products,[20−22] to prioritize selaginellin analogues from the extract and fractions of *S. tamariscina* (P. Beauv.) Spring. Based on the molecular network, chromatographic peaks estimated as previously unknown selaginellin derivatives were prioritized and isolated. As a result, two unusual 1*H*,3*H*-dibenzo[*de*,*h*]isochromene derivatives, selariscins A (**1**) and B (**2**), and eight new diarylfluorene derivatives, selaginpulvilins M−T (**3**−**10**), were identified. The PDE4 inhibitory activities of **1**−**10** were studied in addition to their binding modes.

RESULTS AND DISCUSSION

The 90% EtOH extract of the air-dried roots and rhizophores of *S. tamariscina* and the *n*-hexane, $CHCl_3$, EtOAc, and *n*-

Received: January 18, 2019
Published: June 21, 2019

DOI: 10.1021/acs.jnatprod.9b00049
J. Nat. Prod. 2019, 82, 1820−1830

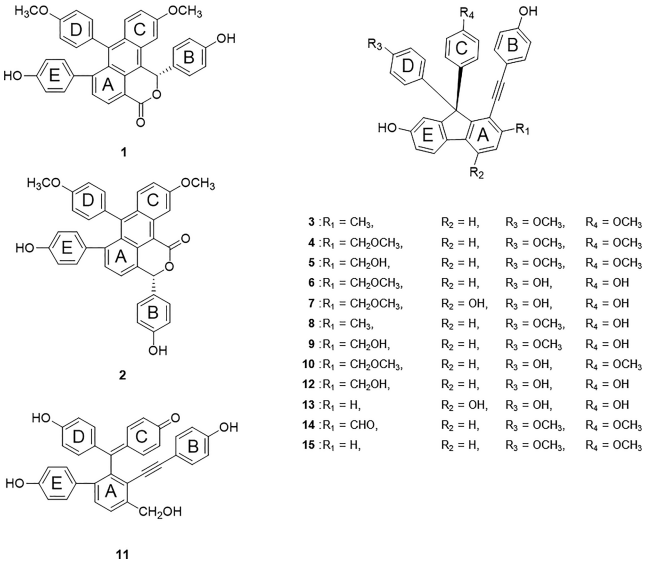

BuOH fractions were prepared and analyzed by LC−MS/MS. Although the MS/MS spectrum of selaginellin (**11**) was not deposited in any accessible MS/MS spectral library, the chromatographic peak of **11** was readily annotated based on its unique molecular formula ($C_{34}H_{24}O_5$). Manual inspection of the MS/MS data of fractions revealed that selaginellin was primarily present in the EtOAc extract. In order to reveal the chemical diversity of minor selaginellin derivatives, the EtOAc extract was further fractionated by silica gel open column chromatography and analyzed by LC−MS/MS. The MS/MS data of subfractions were analyzed by MN via the GNPS Web platform (https://gnps.ucsd.edu) to cluster similar spectra as molecular families (MFs) (Figure 1A).[23,24] In the molecular network, one of the subfractions, namely, E8, showed the largest number of spectral nodes grouped within the same MF as **11**. This MF contained 47 spectral nodes, and most of them were estimated to be selaginellin derivatives, according to their molecular formulas predicted from the precursor ion *m*/*z* values (Figure 1B). Only one spectral node in this MF (precursor ion *m*/*z* 283.060) showed a spectral library match to 4′-*O*-methylgenistein; however, this node and three other nodes of *m*/*z* 333.075, 333.076, and 357.076 showed high mass differences compared to the other nodes, so these were suggested to be false positive results of cosine similarity comparison. An *in silico* fragmentation study supported the assumption that this molecular family contains MS/MS spectral nodes of selaginellin derivatives. The chemical structures of these spectra were estimated using MetFrag,[25] which was coded in the Network Annotation Propagation (NAP) module in GNPS;[26] compound **11** and selaginellins A, B, D, and I were putatively annotated by MetFrag (Figure S1, Supporting Information). However, most other spectral nodes showed candidate structures of totally different classes. We hypothesized that these spectral nodes were not annotated properly because their correct structures do not exist in the chemical libraries, as was demonstrated in our previous study.[27] Hence, we attempted to purify compounds from the subfraction E8, which was expected to contain a number of new selaginellin derivatives. As predicted, further chromatographic separations of the E8 subfraction afforded compounds **1**−**10**, along with known derivatives selaginellin (**11**) and selaginpulvilins A (**12**),[7] I (**13**),[10] K (**14**),[8] and L (**15**).[8]

The molecular formula of selariscin A (**1**) was suggested as $C_{36}H_{26}O_6$ by HRESIMS (*m*/*z* 553.1666 $[M - H]^-$, calcd for $C_{36}H_{25}O_6$, 553.1656), with 24 indices of hydrogen deficiency. The ^{1}H NMR data (Table 1) showed the presence of a 1,2,3,4-tetrasubstituted benzene ring A [δ_H 8.36 and 7.32 (d, J = 7.2 Hz)]; three 1,4-disubstituted benzene rings B [δ_H 7.13 and 6.70 (d, J = 8.7 Hz)], D [δ_H 6.91 (dd, J = 8.3, 2.0 Hz), 6.64 (dd, J = 8.3, 2.6 Hz), 6.61 (dd, J = 8.3, 2.6 Hz), 6.78 (dd, J = 8.3, 2.0 Hz)], and E [δ_H 6.73 (dd, J = 8.2, 1.9 Hz), 6.41 (dd, J = 8.2, 2.4 Hz), 6.37 (dd, J = 8.3, 2.4 Hz), 6.66 (dd, J = 8.3, 1.9 Hz)]; and a 1,2,4-trisubstituted benzene ring C [δ_H 7.30 (d, J = 2.3 Hz), 7.09 (dd, J = 9.7, 2.3 Hz), 7.48 (d, J = 9.7 Hz)]. The ^{1}H−^{1}H COSY spectrum confirmed the cross-peak correlations of benzene rings (Figure 2). In addition to these rings, two methoxy groups [δ_H 3.84 (s) and 3.72 (s)], an oxygenated methine (δ_C/δ_H 79.7/7.76), an upfield-shifted carbonyl (δ_C 164.0), and two sp^2 carbons (δ_C 123.0 and 138.6) were observed. The 1*H*,3*H*-dibenzo[*de*,*h*]isochromene skeleton was established based on the HMBC experiment (Figure 2). Strong HMBC correlations from H-8 (δ_H 7.48) and H-16 (δ_H 6.78) to C-7 (δ_C 138.6) revealed that rings C and D are attached to C-7. The correlation between H-22 (δ_H 6.66) and C-6 (δ_C 148.5) suggested that the E-ring is connected to C-6. The correlations between H-24/28 (δ_H 7.13) and C-1 (δ_C 79.7) showed that the B-ring is attached to the oxygenated methine C-1. The lactone group was located by HMBC correlations from H-4 (δ_H 8.36) and H-1 (δ_H 7.76) to C-3 (δ_C 164.0). HMBC correlations from H-1 (δ_H 7.76) to C-11b (δ_C 123.0) and C-11c (δ_C 126.8) and from H-11 (δ_H 7.30) to C-11b (δ_C 123.0) revealed the isochromene substructure. Thus, the 2D structure of compound **1** was established as shown.

Selariscin B (**2**) was assigned a molecular formula of $C_{36}H_{26}O_6$, the same as **1**. The NMR data of **2** were similar to those of **1** (Table 1), but slight differences in the NMR spectra suggested that compound **2** has a different molecular structure than **1**. The ^{1}H NMR signal of the oxygenated methine (δ_H 6.84, H-3) was significantly upfield shifted versus H-1 of **1**. Chemical shifts of H-4 (δ_H 7.19) and H-11 (δ_H 8.98) were also highly shifted, while the chemical shifts of the carbons to which they were attached were highly similar. This suggested that the lactone ring structure of **2** is different from that of **1**. The oxygenated methine hydrogen (H-3) of **2** showed an HMBC correlation to C-4 (δ_C 124.4), but not to C-11b (δ_C 112.0) (Figure 2). From this, the 2D structure of **2** was assigned as shown in the structural figure. The assigned structure of **2** was interesting because the 1*H*,3*H*-dibenzo[*de*,*h*]isochromene skeleton of compound **1** was estimated to be biosynthesized from selaginellin U.[28] However, no plausible biosynthetic pathway could be established for **2**.

Selaginpulvilin M (**3**) has a molecular formula of $C_{36}H_{28}O_4$ as determined by HRESIMS (*m*/*z* 523.1928 $[M - H]^-$, calcd for $C_{36}H_{27}O_4$, 523.1914). The ^{1}H NMR data (Table 2) revealed the presence of three 1,4-disubstituted aromatic rings B [δ_H 6.84 and 6.72 (2H, d, J = 8.0 Hz)], C [δ_H 7.09 and 6.77 (2H, d, J = 8.4 Hz)], and D [δ_H 7.09 and 6.77 (2H, d, J = 8.4 Hz)]; a 1,2,4-trisubstituted aromatic ring [δ_H 7.65 and 6.74 (1H each, d, J = 8.0 Hz), and 6.61 (s)]; a 1,2,3,4-tetrasubstituted aromatic ring [δ_H 7.28 and 7.67 (1H each, d, J = 7.6 Hz)]; two overlapped methoxy groups [δ_H 3.67 (6H, s)]; and a methyl group [δ_H 2.38 (s)]. The ^{1}H−^{1}H COSY spectrum assigned each aromatic spin system (Figure 2). In addition to these rings, two alkynyl carbons (δ_C 85.3 and 100.8) and an sp^3 quaternary carbon (δ_C 64.2) were observed

DOI: 10.1021/acs.jnatprod.9b00049
J. Nat. Prod. 2019, 82, 1820−1830

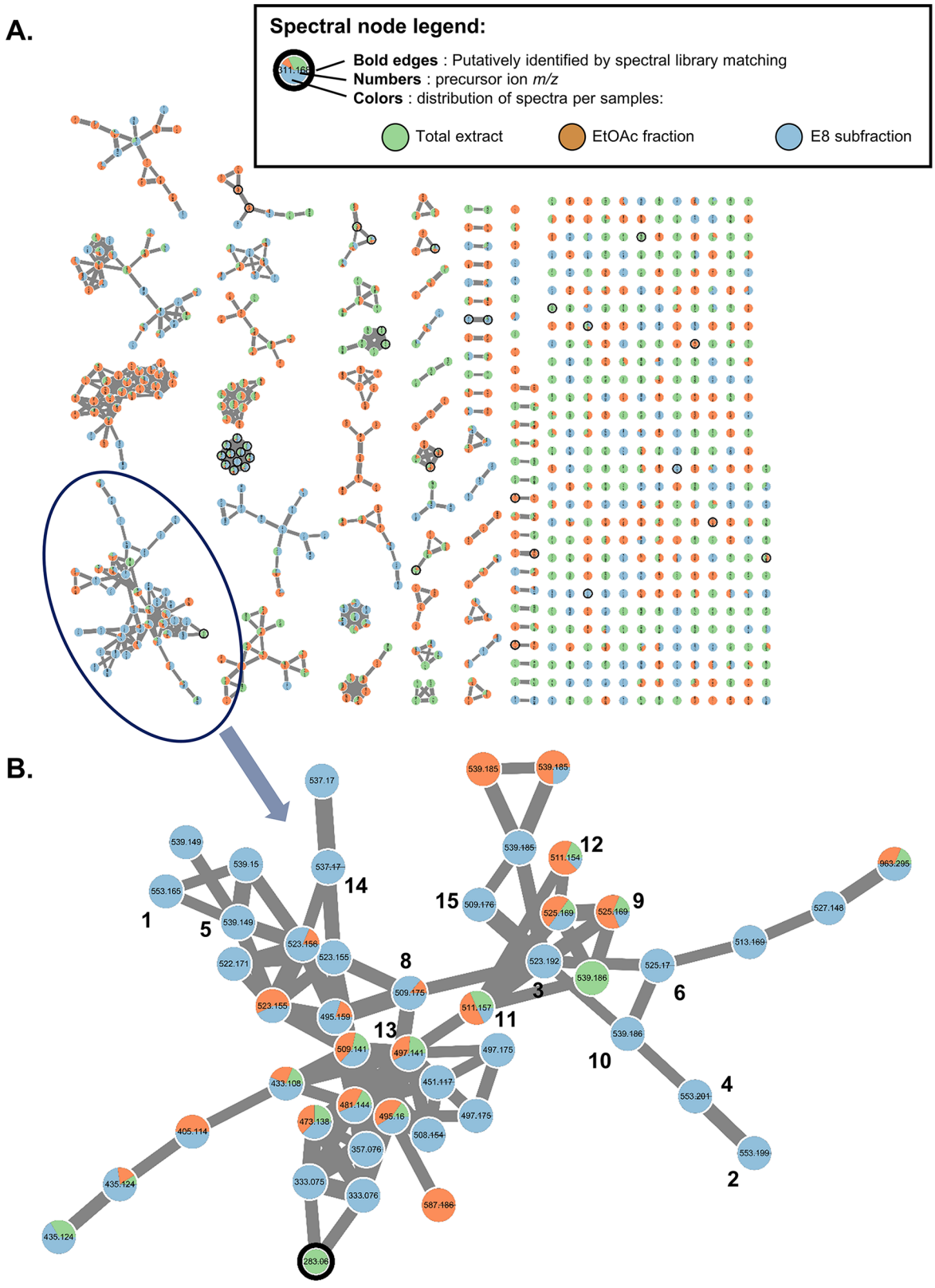

Figure 1. Dereplication strategy for prioritization of selaginellin derivatives using MS/MS molecular networking: (A) entire molecular network of *S. tamariscina* extract and fractions; (B) targeted isolation of selaginellin derivatives within the selected molecular family.

in the ^{13}C NMR spectrum (Table 3). These results suggested that compound **3** is one of the selaginpulvilin analogues and is especially similar to **14**. The HMBC experiment confirmed that compound **3** has a methyl group at C-2 instead of the formyl group of **14** (Figure 2). Selaginpulvilins N and O (**4** and **5**) also showed similar spectra to **3**, and they were identified to have a methoxymethyl and a hydroxymethyl group at C-2, respectively. Selaginpulvilin P (**6**) showed NMR

DOI: 10.1021/acs.jnatprod.9b00049
J. Nat. Prod. 2019, 82, 1820−1830

Table 1. ^{1}H, ^{13}C, and HMBC NMR Spectroscopic Data of Compounds 1 and 2 (600/150 MHz, in DMSO-d_6)

	1			2		
position	δ_H	δ_C	HMBC	δ_H	δ_C	HMBC
1	7.76, s	79.7	C-11b, C-11c, C-3, C-24, C-29		164.9	
3		164.0		6.84, br s	79.5	C-11c, C-1, C-4, C-28
3a		125.7			125.8	
4	8.36, d (7.2)	129.3	C-11c, C-3, C-6	7.19, dd (7.1, 1.1)[a]	124.4	C-3, C-3a,[b] C-11c, C-6
5	7.32, d (7.2)	129.2	C-3a, C-6a, C-23	7.14, d (7.1)	129.0[a]	C-3a, C-6a, C-23
6		148.5			141.5	
6a		118.3			129.8[a]	
7		138.6			146.7	
7a		127.8			128.3	
8	7.48, d (9.7)	129.7	C-7, C-11a, C-10	7.49, d (9.7)	129.8[a]	C-7, C-11a, C-10
9	7.09, dd (9.7, 2.3)	120.3	C-7a, C-11	7.17, dd (9.7, 2.6)[a]	120.1	C-7a, C-11
10		157.7			159.9	
11	7.30, d (2.3)	100.1	C-11b, C-7a, C-10, C-9	8.98, d (2.6)	102.8	C-11b, C-7a, C-10, C-9
11a		128.1			133.4	
11b		123.0			112.0	
11c		126.8			131.0	
12	6.91, dd (8.3, 2.0)	133.0	C-7, C-14, C-16	6.86[a]	132.6	C-7, C-14, C-16
13	6.64, dd (8.3, 2.6)	113.0	C-15, C-17	6.64[a]	113.0[a]	C-14, C-15, C-17
14		158.0			158.2	
15	6.61, dd (8.3, 2.6)	113.1	C-13, C-17	6.62[a]	113.0[a]	C-14, C-13, C-17
16	6.78, dd (8.3, 2.0)	132.9	C-7, C-12, C-14	6.80[a]	132.5	C-7, C-12, C-14
17		130.9			130.9	
18	6.73, dd (8.2, 1.9)	130.0	C-6, C-20, C-22	6.60, d (8.6)	130.5[a]	C-6, C-20, C-22
19	6.41, dd (8.2, 2.4)	114.1	C-21, C-23	6.35, dd (8.1, 4.9)	113.9	C-21, C-23
20		155.7			155.3	
21	6.37, dd (8.3, 2.4)	114.0	C-19, C-23	6.35, dd (8.1, 4.9)	113.9	C-19, C-23
22	6.66, dd (8.3, 1.9)	130.5	C-6, C-18, C-20	6.60, d (8.6)	130.4[a]	C-6, C-20, C-18
23		133.6			133.7	
24	7.13, d (8.7)	128.9	C-1, C-26, C-28	7.24, d (8.6)	129.0[a]	C-3, C-26, C-28
25	6.70, d (8.7)	115.8	C-27, C-26, C-29	6.80, d (8.6)[a]	115.5	C-27, C-29
26		158.0			157.9	
27	6.70, d (8.7)	115.8	C-25, C-26, C-29	6.80, d (8.6)[a]	115.5	C-27, C-29
28	7.13, d (8.7)	128.9	C-1, C-24, C-26	7.24, d (8.6)	129.0[a]	C-5, C-26, C-24
29		131.2			129.6	
10-OCH_3	3.84, s	55.5	C-10	3.96, s	55.4	C-10
14-OCH_3	3.72, s	55.2	C-14	3.72, s	55.2	C-14

[a]Overlapped. [b]Weak correlation.

spectra similar to **12**,[7] with the replacement of the hydroxymethyl group at C-2 by a methoxymethyl group. The NMR spectra of selaginpulvilin Q (**7**) (Tables 2 and 3) were similar to those of **13**,[10] but the differences between the spectra of **7** and **13** suggested that compound **7** possesses a methoxymethyl group at C-2. The 2D structure of selaginpulvilin R (**8**) was elucidated as shown, which is similar to compound **3**. However, one of the methoxy groups of the C- and D-rings of **3** is replaced with a hydroxy group, and this caused asymmetry of the C- and D-rings. Selaginpulvilins S and T (**9** and **10**) were also characterized as asymmetric derivatives, and so the absolute configurations of compounds **8**−**10** had to be resolved.

Despite extensive efforts, compounds **1**, **2**, and **8**−**10** could not be crystallized for X-ray diffraction data collection. Alternatively, computational electronic circular dichroism (ECD) analysis was utilized to determine the absolute configurations at C-1 of **1**, C-3 of **2**, and C-9 of **8**−**10**. By comparison of the experimental and calculated ECD data, the absolute configuration of C-1 of **1** was assigned as *S* (Figure 3). In detail, the positive Cotton effects in the calculated ECD spectra of **1**, at approximately 248 and 331 nm, arise from the electronic transition from aromatic π orbitals and a lone-pair oxygen orbital to aromatic π^* orbitals and a carbonyl π^* orbital (MO 145 → 147 and MO 138 → 147). This band could be correlated to the Cotton effects at 255 and 333 nm in the experimental ECD curve (Figure 3). In addition, the negative Cotton effects at 240 and 310 nm in the experimental curves were also reproduced by the calculations at 236 and 306 nm, respectively (Figure 3). The electronic transitions from aromatic π orbitals to aromatic π^* orbitals contributed to these absorption bands (MO 145 → 149 and MO 144 → 154) (Figure S78 and Table S8, Supporting Information). Similarly, the absolute configurations at C-3 in **2** and C-9 in **8**−**10** were assigned as *R*, *R*, *R*, and *S*, respectively, by comparison of the experimental and calculated ECD spectra (Figure 3, Figure S83 and Table S9, Supporting Information).

PDE4 comprises four subfamilies, PDE4A, PDE4B, PDE4C, and PDE4D.[29] Among them, previous studies reported that selaginellin (**11**) and selaginpulvilin derivatives exhibit potent inhibition against PDE4D2, one of the splicing variants of PDE4D. Compounds **11**−**15** showed IC_{50} values of 1.0 μM

DOI: 10.1021/acs.jnatprod.9b00049
J. Nat. Prod. 2019, 82, 1820−1830

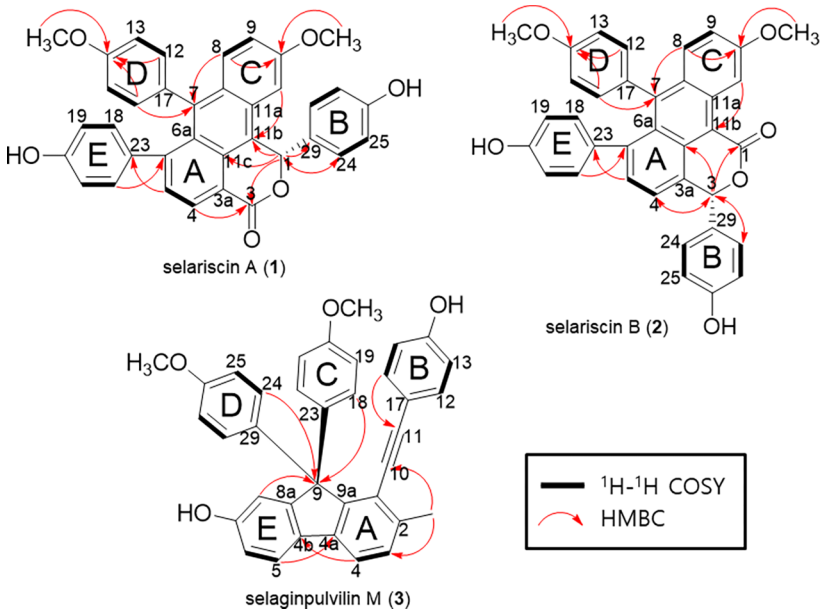

Figure 2. Key ^{1}H−^{1}H COSY and key HMBC correlations of compounds **1**−**3**.

Table 2. ^{1}H NMR Spectroscopic Data (δ_H in ppm) of Compounds 3−10 (in DMSO-d_6)

position	3[b]	4[b]	5[b]	6[b]	7[c]	8[b]	9[c]	10[b]
3	7.28, d (7.6)	7.42, d (7.9)	7.51, d (7.8)	7.40, d (7.9)	6.95, br s	7.27, d (7.8)	7.50, d (7.9)	7.41, d (7.8)
4	7.67, d (7.6)	7.76, d (7.9)	7.77, d (7.8)	7.73, d (7.9)		7.65, d (7.8)	7.75, d (7.9)	7.74, d (7.8)
5	7.65, d (8.0)	7.69, d (8.3)	7.67, d (8.2)	7.66, d (8.2)	7.82, d (8.3)	7.63, d (8.2)	7.65, d (8.2)	7.67, d (8.2)
6	6.74, d (8.0)	6.76[a]	6.75, dd (8.2, 2.0)	6.75, dd (8.2, 2.1)[a]	6.68, dd (8.3, 2.2)	6.74, dd (8.2, 2.0)[a]	6.74, dd (8.2, 2.1)[a]	6.74, dd (8.2, 2.1)[a]
8	6.61, s	6.62, s	6.62, d (2.0)	6.63, d (2.1)	6.58, d (2.2)	6.61, d (2.0)	6.62, d (2.1)	6.62, d (2.1)
12	6.84, d (8.0)	6.85, d (8.5)	6.83, d (8.5)	6.89, d (8.5)	6.83, d (8.5)	6.86, d (8.5)	6.85, d (8.6)	6.86, d (8.5)
13	6.72, d (8.0)	6.73, d (8.5)	6.72, d (8.5)	6.74, d (8.5)[a]	6.70, d (8.5)	6.72, d (8.5)[a]	6.72, d (8.6)	6.73, d (8.5)
15	6.72, d (8.0)	6.73, d (8.5)	6.72, d (8.5)	6.74, d (8.5)[a]	6.70, d (8.5)	6.72, d (8.5)[a]	6.72, d (8.6)	6.73, d (8.5)
16	6.84, d (8.0)	6.85, d (8.5)	6.83, d (8.5)	6.89, d (8.5)	6.83, d (8.5)	6.86, d (8.5)	6.85, d (8.6)	6.86, d (8.5)
18	7.09, d (8.4)	7.09, d (8.9)	7.09, d (8.9)	6.97, d (8.8)	6.97, d (8.8)	6.98, d (8.8)	6.98, d (8.8)	7.09, d (8.9)
19	6.77, d (8.4)	6.77, d (8.9)[a]	6.77, d (8.9)	6.57, d (8.8)	6.55, d (8.8)	6.58, d (8.8)	6.58, d (8.8)	6.76, d (8.9)[a]
21	6.77, d (8.4)	6.77, d (8.9)[a]	6.77, d (8.9)	6.57, d (8.8)	6.55, d (8.8)	6.58, d (8.8)	6.58, d (8.8)	6.76, d (8.9)[a]
22	7.09, d (8.4)	7.09, d (8.9)	7.09, d (8.9)	6.97, d (8.8)	6.97, d (8.8)	6.98, d (8.8)	6.98, d (8.8)	7.09, d (8.9)
24	7.09, d (8.4)	7.09, d (8.9)	7.09, d (8.9)	6.97, d (8.8)	6.97, d (8.8)	7.09, d (8.9)	7.09, d (9.0)	6.97, d (8.8)
25	6.77, d (8.4)	6.77, d (8.9)[a]	6.77, d (8.9)	6.57, d (8.8)	6.55, d (8.8)	6.76, d (8.9)	6.75, d (9.0)[a]	6.58, d (8.8)
27	6.77, d (8.4)	6.77, d (8.9)[a]	6.77, d (8.9)	6.57, d (8.8)	6.55, d (8.8)	6.76, d (8.9)	6.75, d (9.0)[a]	6.58, d (8.8)
28	7.09, d (8.4)	7.09, d (8.9)	7.09, d (8.9)	6.97, d (8.8)	6.97, d (8.8)	7.09, d (8.9)	7.09, d (9.0)	6.97, d (8.8)
30	2.38, s	4.52, s	4.63, s	4.53, s	4.46, s	2.37, s	4.64, s	4.52, s
30-OCH_3		3.34, s		3.35, s	3.34, s			3.35, s
20-OCH_3	3.67, s	3.67, s	3.67, s					
26-OCH_3	3.67, s	3.67, s	3.67, s			3.66, s	3.67, s	3.67, s

[a]Overlapped. [b]Recorded at 850 MHz. [c]Recorded at 800 MHz.

DOI: 10.1021/acs.jnatprod.9b00049
J. Nat. Prod. 2019, 82, 1820−1830

Table 3. ^{13}C NMR Spectroscopic Data of Compounds 3−10 (in DMSO-d_6)

position	3[b]	4[b]	5[b]	6[b]	7[c]	8[b]	9[c]	10[b]
1	120.4	119.6	117.9	119.6	109.4	120.5	118.0	119.6
2	137.4	137.5	141.9	137.4	139.0	137.5	141.8	137.4
3	128.9	127.7	125.9	127.3	114.0	128.9	125.7	127.4
4	118.8	118.9	118.7	118.6	152.7	118.9	118.6	118.6
4a	138.5	140.2	139.2	140.1	126.1	138.5	139.2	140.1
4b	129.8	129.6	129.7[a]	129.5	129.4	130.0	129.7[a]	129.4
5	120.9	121.4	121.0	121.1	123.7	121.0	120.8	121.1
6	114.8	115.1	114.9	114.8	114.1	114.9	114.7	114.9
7	157.9	158.3	158.0	158.1	156.8	157.9[a]	157.9	158.2
8	112.0	112.1	112.0	112.0	111.8	112.1	112.0	112.0
8a	155.3	155.7	155.4	156.0	155.2	155.6	155.6	155.8
9	64.2	64.3	64.2	64.3	64.5	64.4	64.2	64.2
9a	151.2	151.2	150.9	151.6	157.8	151.6	151.1	151.3
10	85.3	84.2	84.0	84.2	84.5	85.5	84.0	84.1
11	100.8	100.9	101.1	100.7	98.1	100.8	101.0	100.9
12	132.3	132.5	132.3	132.3	131.8	132.4	132.2	132.3
13	115.8	115.9	115.8	115.8	115.7	115.9	115.7	115.9
14	158.3	158.5	158.4	158.4	157.9	158.3	158.3	158.6
15	115.8	115.9	115.8	115.8	115.7	115.9	115.7	115.9
16	132.3	132.5	132.3	132.3	131.8	132.4	132.2	132.3
17	112.7	112.7	112.6	112.7	113.2	113.1	112.7	112.3
18	129.7	129.8	129.7[a]	129.7	129.7	129.9	129.7[a]	129.7[a]
19	113.1	113.2	113.1	114.3	114.2	114.5	114.3	113.0
20	157.8	158.0	157.8	156.0	155.8	156.1	156.0	157.8
21	113.1	113.2	113.1	114.3	114.2	114.5	114.3	113.0
22	129.7	129.8	129.7[a]	129.7	129.7	129.9	129.7[a]	129.7[a]
23	134.5	134.4	134.5	132.7	132.9	132.8	132.5	134.6
24	129.7	129.8	129.7[a]	129.7	129.7	129.9	129.7[a]	129.7[a]
25	113.1	113.2	113.1	114.3	114.2	113.1	113.0	114.4
26	157.8	158.0	157.8	156.0	155.8	157.9[a]	157.7	156.1
27	113.1	113.2	113.1	114.3	114.2	113.1	113.0	114.4
28	129.7	129.8	129.7[a]	129.7	129.7	129.9	129.7[a]	129.7[a]
29	134.5	134.4	134.5	132.7	132.9	134.9	134.7	132.4
30	20.6	72.3	61.3	72.3	72.1	20.7	61.3	72.2
30-OCH_3		55.2		58.1	58.0			58.1
20,26-OCH_3	55.1	58.2	55.1			55.2	55.0	55.0

[a]Overlapped. [b]Recorded at 850/212.5 MHz. [c]Recorded at 200 MHz.

(**11**), 0.2 μM (**12**), 1.2 μM (**13**), 10 nM (**14**), and 90 nM (**15**), while the positive control rolipram exhibited an IC_{50} of 0.5−0.6 μM.[7,8,10] The inhibitory activity of compounds **1**−**10** was also evaluated against human PDE4D2. Compounds **1** and **3**−**10** showed inhibitory activity with IC_{50} values in the range of 2.8−33.8 μM, while rolipram exhibited an IC_{50} of 0.2 μM (Table 4). The dose−response curves of **1** and **3**−**10** are represented in Figure S86 (Supporting Information). Interestingly, compound **2** did not inhibit PDE4D2, although **1** and **2** have the same scaffold. This suggests that the position of the B-ring in these selaginellin analogues has an important impact on the inhibitory potency against PDE4. Previous structure−activity relationship (SAR) studies on selaginpulvilin derivatives revealed that 20,26-OCH_3 groups are important for inhibitory activity against PDE4D2.[8] Our results agreed with this conclusion, as compounds **4** and **5**, which have *p*-methoxyphenyl C and D rings, were significantly more potent than compounds **6**−**10**. However, compound **3** showed weaker inhibition, although it contains methoxy groups at C-20 and C-26. This suggests that the substitution at C-2 could affect the PDE4 inhibitory activity of selaginpulvilin derivatives.

To further investigate the interactions between these selaginellin derivatives and PDE4D2, molecular docking studies were carried out to explore the binding modes. In order to establish the putative binding modes of **1** and **3**−**10** in the active site of human PDE4D2, molecular docking was simulated using the CDOCKER algorithm.[30] As shown in Figure 4 and Figures S91−S93 (Supporting Information), **1**−**15** bound to the active sites of the PDE4D2 catalytic domain, and their E-ring hydroxy group formed hydrogen bonds with the His160 residue or metals (zinc and magnesium), mediated by water molecules. Compounds **1**, **3**−**5**, **7**−**11**, and **13**−**15** interacted with the Phe372 residue, forming $\pi-\pi$-stacked or $\pi-\pi$ T-shaped interactions. The π-stacking interaction against the conserved phenylalanine residues (Phe372 in PDE4D) located in the active site is a common interaction observed in other PDE4 inhibitors.[31,32] Furthermore, compounds **1**, **3**, **4**, **5**, and **8**, showing relatively low IC_{50} values, also interacted with Met273, Met357, and Ile336 residues via π-alkyl hydrophobic interactions (Figure 4A, C, and D; Figure S87, Supporting Information). On the other hand, compound **2** showed unfavorable donor−donor interactions with Ser227 and Ser274 residues only (Figure 4B). This explained the reason

DOI: 10.1021/acs.jnatprod.9b00049
J. Nat. Prod. 2019, 82, 1820−1830

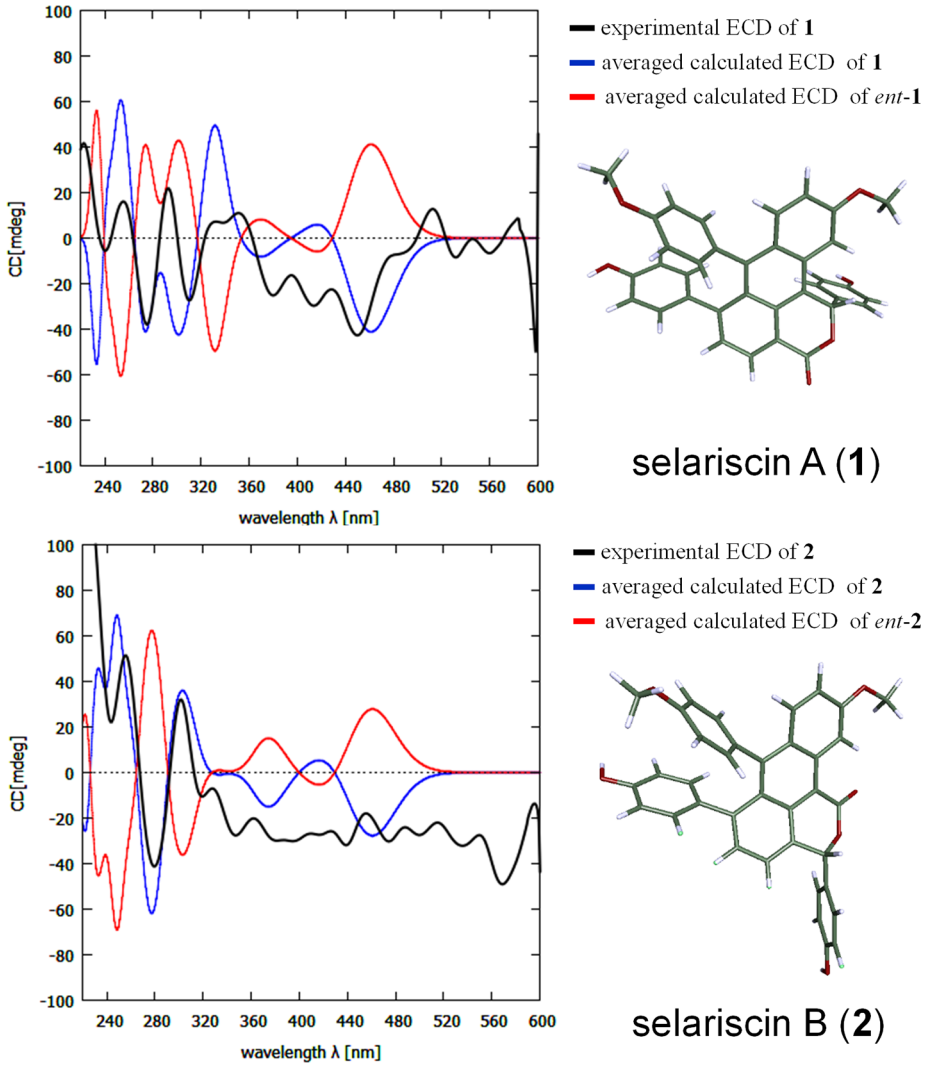

Figure 3. Comparison between the experimental and Bolzmann-averaged calculated ECD spectra of **1** and **2**. The structures show energy-minimized structures of the lowest-energy conformers.

Table 4. Inhibitory Activity of Compounds 1−10 against PDE4D2

compound	IC_{50} (μM)	95% confidence interval
1	13.7	8.9−40.2
2	>30	
3	24.6	14.3−246.0
4	2.8	2.3−3.4
5	5.4	4.3−6.8
6	23.2	19.1−32.4
7	29.5	19.0−117.4
8	19.5	15.8−25.8
9	32.1	19.7−205.5
10	33.8	24.6−96.8
rolipram[a]	0.2	0.2−0.2

[a]Positive control.

that compound **2** was inactive while **1** showed moderate activity. We could not find a significant difference in the binding interaction between compounds **3**, and **4** and **5**; however, we presume that the relatively large and stretched skeleton could render selaginpulvilins more highly selective for PDE4D2. Unlike other active compounds, compound **6** did not display a close interaction with Phe372 but showed interactions with other residues such as Gln210 and Cys358. This suggests that there might be other residues affecting the inhibitory activity against PDE4D2. Taken together, the high number of favorable interactions and absence of unfavorable interactions in **1**, **3**, **4**, **5**, **6**, and **8** are responsible for their binding affinities.

This study demonstrated that MS/MS molecular networking is a promising tool for seeking natural molecules with a certain scaffold of interest, even in the case where one does not have any previously obtained derivative or reference spectrum. Recent advances in computational MS/MS spectra annotation tools allow for automated, massive dereplication for natural product data sets, as shown in this study and other recent studies.[27,33,34] It is anticipated that this next-generation MS/MS data analysis workflow combined with public spectra deposits will accelerate structure-based natural product discovery in the scientific community. This approach led to the isolation of 10 selaginellin derivatives from *S. tamariscina*. Among them, selariscins A (**1**) and B (**2**) are the first naturally occurring 1*H*,3*H*-dibenzo[*de*,*h*]isochromene derivatives. The MS/MS spectra of isolated compounds were deposited in the publicly accessible GNPS spectral library. This will allow every

DOI: 10.1021/acs.jnatprod.9b00049
J. Nat. Prod. 2019, 82, 1820−1830

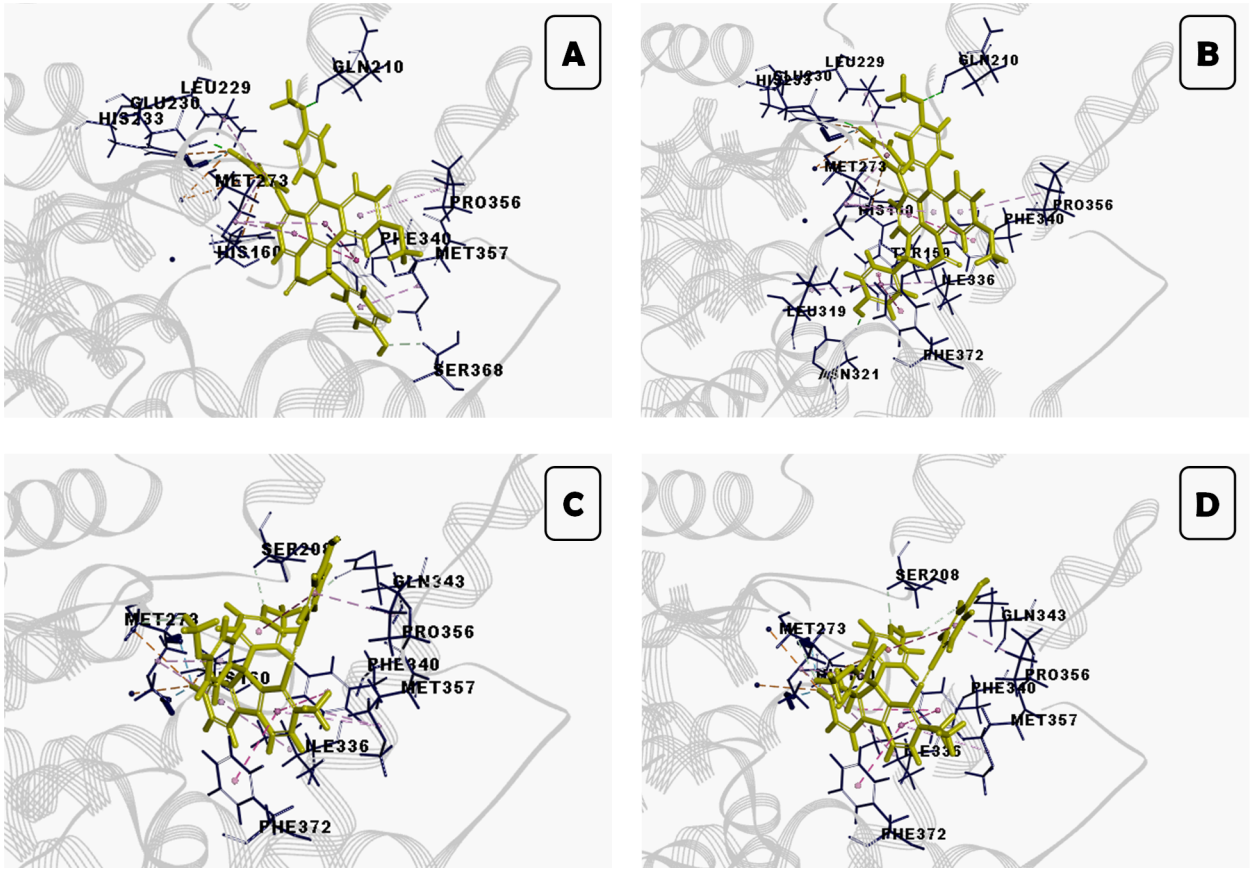

Figure 4. Predicted binding modes of compounds **1** (A), **2** (B), **3** (C), and **4** (D) against human PDE4D2 derived from docking simulations.

natural product chemist to detect these compounds and analogues. Moreover, the isolated compounds were evaluated for their PDE4D2 inhibitory activity, and their binding modes were suggested based on the molecular docking study. These results will contribute to PDE4 inhibitor development based on selaginellin scaffolds.

EXPERIMENTAL SECTION

General Experimental Procedures. Optical rotations were measured on a JASCO P-2000 polarimeter (JASCO, Tokyo, Japan) using a 1 cm cell at 20 °C using a sodium lamp (589 nm). ECD and UV spectra were recorded on a Chirascan CD spectrometer (Applied Photophysics, Surrey, UK). 1D and 2D NMR spectra were recorded on a Bruker Avance III HD 800 MHz, 850 MHz, or Avance III 600 MHz spectrometer (Bruker, Billerica, MA, USA) equipped with a 5 mm TCI cryoprobe. The measurement temperature was 290 K. HRESIMS and MS/MS analyses were performed with a Waters XEVO G2 Q-TOF MS (Waters MS Technologies, Manchester, UK), which was equipped with an electrospray ionization (ESI) interface. Column chromatography (CC) was performed with Zeoprep 60 silica gel (60−200 μm, Zeochem, Uetikon am See, Switzerland). Preparative HPLC separations were performed using a Gilson 321 pump and a Gilson UV/vis-151 detector (Gilson Inc., Middleton, WI, USA), equipped with an XBridge BEH C_{18} OBD Prep column (19 mm × 250 mm, 5 μm, Waters, Wexford, Ireland) or a YMC Triart C_{18} column (10 mm × 250 mm, 5 μm, YMC, Kyoto, Japan). Extra-pure grade solvents for extraction, fractionation, and isolation were purchased from Daejung Chemical & Metal Co., Ltd. (Siheung, Korea). HPLC grade water and MeCN were purchased from J.T. Baker (Avantor, Phillipsburg, NJ, USA), and formic acid was acquired from Sigma-Aldrich (St. Louis, MO, USA). Deuterated solvents for NMR analysis were purchased from Cambridge Isotope Laboratories (Cambridge, MA, USA).

Plant Materials. The air-dried roots of *S. tamariscina* (P. Beauv.) Spring were collected in Yeongcheon, Gyeongsangbuk-do, Korea (GPS N 36°01′09″, E 128°56′16″), in June 2015. The collected plant samples were authenticated by Prof. Tae-Jin Yang (College of Agricultural and Life Sciences, Seoul National University). A voucher specimen (SUPH-1506-01) is deposited in the Herbarium of the Medicinal Plant Garden, College of Pharmacy, Seoul National University, Koyang, Korea.

MS/MS Molecular Networking. The total extract and fractions were analyzed by LC−MS/MS equipped with a Waters Acquity UPLC BEH C_{18} (100 mm × 2.1 mm, 1.7 μm) column, of which the temperature was maintained at 40 °C. Mixtures of H_2O (A) and MeCN (B) were eluted at the flow rate of 0.3 mL/min with a linear gradient of 10−100% B (0−17 min). The samples (2 mg/mL total extract, 1 mg/mL subfractions; 1.0 μL portions were injected) were analyzed in data-dependent acquisition (DDA) mode: The full MS survey scan was performed for 150 ms in the range of 100−2000 Da; then the three most intense ions were further scanned for MS/MS fragmentation spectra. The gradient of collision energy was set as 20 to 80 V. The MS/MS data were converted to the .mzXML format with MS-Convert[35] and then uploaded on the GNPS Web platform (https://gnps.ucsd.edu) for molecular networking. The MS/MS molecular network was generated using the GNPS "Classic" molecular networking workflow (METABOLOMICS-SNETS-V2), in which the MS-Cluster[36] is activated. Parameters for molecular network generation were set as follows: precursor mass tolerance m/z 0.02 Da, MS/MS fragment ion tolerance m/z 0.02 Da, minimum cosine score 0.7, minimum matched fragment ions 4, minimum cluster size 2, network TopK 10. The spectral library matching was performed with the same minimum cosine score and matched fragment ion number filtering parameter. The generated molecular network was visualized using Cytoscape 3.5.1. MetFrag *in silico* fragmentor analysis was performed by using NAP workflow (https://proteomics2.ucsd.edu/ProteoSAFe/?params={%22workflow%22:%22NAP_CCMS2%22}),

DOI: 10.1021/acs.jnatprod.9b00049
J. Nat. Prod. 2019, 82, 1820−1830

in which candidate structures were searched with the exact mass filter of 5 ppm from the structural databases of DNP, GNPS, and SuperNatural. Raw MS/MS data were deposited in the MassIVE Public GNPS data sets (https://massive.ucsd.edu) with accession no. MSV000083197. The MS/MS molecular network and NAP annotation are accessible at the GNPS Web site with the following links:

https://gnps.ucsd.edu/ProteoSAFe/status.jsp?task=885c88d84d624f778fd8ca5aa968ce99

https://proteomics2.ucsd.edu/ProteoSAFe/status.jsp?task=9e4ffe2d0897413cb83600e1a8183aea

Extraction and Isolation. Air-dried powder of the roots and rhizophores of *S. tamariscina* (8.4 kg) was extracted with 90% EtOH (3 × 84 L, for 2 h each) using an ultrasonicator at room temperature. A 366.2 g amount of crude extract was obtained after removing the extraction solvent *in vacuo*. The extract was suspended in H_2O and successively partitioned to produce *n*-hexane (30.5 g), $CHCl_3$ (46.6 g), EtOAc (33.7 g), and *n*-BuOH extracts (18.8 g), respectively. The EtOAc extract was subjected to silica gel CC using gradient mixtures of $CHCl_3$ and MeOH (40:1 → 0:100) to afford 14 fractions (E1–E14) by TLC analysis. E8 (1.57 g, eluted when the ratio of $CHCl_3$–MeOH was about 19:1) was separated using preparative HPLC (Waters XBridge C_{18} column, MeCN–H_2O, 36:64 → 100:0, v/v, 15 mL/min, 254 nm) to afford **3** (3.6 mg, t_R 22.0 min) and seven subfractions (E8a–E8g). E8f (113.4 mg) was further purified using semipreparative HPLC (YMC Triart C_{18} column, MeOH–H_2O, 67:33, 3.5 mL/min, 254 nm) to yield **1** (1.2 mg, t_R 15.1 min), **8** (3.6 mg, t_R 12.9 min), and **14** (2.7 mg, t_R 13.8 min). E8g (21.8 mg) was separated by semipreparative HPLC (YMC Triart C_{18} column, MeOH–H_2O, 60:40, 3.0 mL/min, 254 nm) to give **2** (2.0 mg, t_R 43.8 min), **4** (5.5 mg, t_R 26.1 min), and **15** (2,1 mg, t_R 34.5 min). E9 (324.9 mg) was separated using preparative HPLC (Waters XBridge C_{18} column, CH_3CN–H_2O, 36:64 → 100:0, 15 mL/min, 254 nm) to afford **11** (42.5 mg, t_R 7.3 min) and **12** (3.4 mg, t_R 9.0 min). E11 (494.2 mg) was separated using preparative HPLC (Waters XBridge C_{18} column, MeCN–H_2O, 40:60 → 100:0, 12 mL/min, 254 nm) to afford 15 subfractions (E11a–E11o). E11c (73.2 mg) was further purified on semipreparative HPLC (YMC Triart C_{18} column, MeCN–H_2O, 38:62, 3.0 mL/min, 254 nm) to yield **7** (1.9 mg, t_R 31.5 min) and **13** (2.6 mg, t_R 35.0 min). E11g (41.2 mg) was separated by semipreparative HPLC (YMC Triart C_{18} column, MeOH–H_2O, 68:32, 4.0 mL/min, 254 nm) to give **9** (2.7 mg, t_R 10.2 min). E11h (12.9 mg) was separated by semipreparative HPLC (YMC Triart C_{18} column, MeOH–H_2O, 70:30 → 80:20, 4.0 mL/min, 254 nm) to give **6** (4.0 mg, t_R 8.0 min). E11j (12.9 mg) was separated by semipreparative HPLC (YMC Triart C_{18} column, MeOH–H_2O, 75:25, 4.0 mL/min, 254 nm) to give **5** (1.7 mg, t_R 9.1 min) and **10** (1.1 mg, t_R 12.9 min).

*Selariscin A (**1**):* yellow oil; $[\alpha]_D^{20}$ +6 (*c* 0.8, MeOH); UV (MeOH) λ_{max} (log ε) 283 (4.42), 377 (3.40), 428 (3.47) nm; ECD (MeOH) λ_{max} ($\Delta\varepsilon$) 237 (−1.9), 251 (12.5), 288 (−18.8), 346 (1.6) nm; ^{1}H and ^{13}C NMR, see Table 1; HRESIMS *m*/*z* 553.1666 $[M - H]^-$ (calcd for $C_{36}H_{25}O_6$, 553.1656); the MS/MS spectrum is deposited in the GNPS spectral library, https://gnps.ucsd.edu/ProteoSAFe/gnpslibraryspectrum.jsp?SpectrumID=CCMSLIB00004722188#%7B%7D.

*Selariscin B (**2**):* yellow oil; $[\alpha]_D^{20}$ +6 (*c* 1.0, MeOH); UV (MeOH) λ_{max} (log ε) 231 (4.44), 283 (4.55), 382 (3.63), 435 (3.58) nm; ECD (MeOH) λ_{max} ($\Delta\varepsilon$) 278 (−0.6), 308 (12.6) nm; ^{1}H and ^{13}C NMR, see Table 1; HRESIMS *m*/*z* 553.1667 $[M - H]^-$ (calcd for $C_{36}H_{25}O_6$, 553.1656); the MS/MS spectrum is deposited in the GNPS spectral library, https://gnps.ucsd.edu/ProteoSAFe/gnpslibraryspectrum.jsp?SpectrumID=CCMSLIB00004722189#%7B%7D.

*Selaginpulvilin M (**3**):* yellow oil; UV (MeOH) λ_{max} (log ε) 286 (4.47), 300 (4.49) nm; ^{1}H and ^{13}C NMR, see Tables 2 and 3; HRESIMS *m*/*z* 523.1928 $[M - H]^-$ (calcd for $C_{36}H_{27}O_4$, 523.1914); the MS/MS spectrum is deposited in the GNPS spectral library, https://gnps.ucsd.edu/ProteoSAFe/gnpslibraryspectrum.jsp?SpectrumID=CCMSLIB00004722186#%7B%7D.

*Selaginpulvilin N (**4**):* yellow oil; UV (MeOH) λ_{max} (log ε) 301 (4.32) nm; ^{1}H and ^{13}C NMR, see Tables 2 and 3; HRESIMS *m*/*z* 553.2017 $[M - H]^-$ (calcd for $C_{37}H_{29}O_5$, 553.2020); the MS/MS spectrum is deposited in the GNPS spectral library, https://gnps.ucsd.edu/ProteoSAFe/gnpslibraryspectrum.jsp?SpectrumID=CCMSLIB00004722187#%7B%7D.

*Selaginpulvilin O (**5**):* yellow oil; UV (MeOH) λ_{max} (log ε) 289 (4.21), 300 (4.21) nm; ^{1}H and ^{13}C NMR, see Tables 2 and 3; HRESIMS *m*/*z* 539.1848 $[M - H]^-$ (calcd for $C_{36}H_{27}O_5$, 539.1863); the MS/MS spectrum is deposited in the GNPS spectral library, https://gnps.ucsd.edu/ProteoSAFe/gnpslibraryspectrum.jsp?SpectrumID=CCMSLIB00004722196#%7B%7D.

*Selaginpulvilin P (**6**):* yellow oil; UV (MeOH) λ_{max} (log ε) 290 (4.01), 298 (4.05) nm; ^{1}H and ^{13}C NMR, see Tables 2 and 3; HRESIMS *m*/*z* 525.1694 $[M - H]^-$ (calcd for $C_{35}H_{25}O_5$, 525.1707); the MS/MS spectrum is deposited in the GNPS spectral library, https://gnps.ucsd.edu/ProteoSAFe/gnpslibraryspectrum.jsp?SpectrumID=CCMSLIB00004722191#%7B%7D.

*Selaginpulvilin Q (**7**):* yellow oil; UV (MeOH) λ_{max} (log ε) 289 (4.06) nm; ^{1}H and ^{13}C NMR, see Tables 2 and 3; HRESIMS *m*/*z* 541.1656 $[M - H]^-$ (calcd for $C_{35}H_{25}O_6$, 541.1656); the MS/MS spectrum is deposited in the GNPS spectral library, https://gnps.ucsd.edu/ProteoSAFe/gnpslibraryspectrum.jsp?SpectrumID=CCMSLIB00004722190#%7B%7D.

*Selaginpulvilin R (**8**):* yellow oil; $[\alpha]_D^{20}$ −3.5 (*c* 1.0, MeOH); UV (MeOH) λ_{max} (log ε) 287 (4.57), 300 (4.58) nm; ECD (MeOH) λ_{max} ($\Delta\varepsilon$) 244 (1.4), 281 (33.2), 301 (32.8), 322 (6.9) nm; ^{1}H and ^{13}C NMR, see Tables 2 and 3; HRESIMS *m*/*z* 509.1754 $[M - H]^-$ (calcd for $C_{35}H_{25}O_4$, 509.1758); the MS/MS spectrum is deposited in the GNPS spectral library, https://gnps.ucsd.edu/ProteoSAFe/gnpslibraryspectrum.jsp?SpectrumID=CCMSLIB00004722194#%7B%7D.

*Selaginpulvilin S (**9**):* yellow oil; $[\alpha]_D^{20}$ −52 (*c* 1.0, MeOH); UV (MeOH) λ_{max} (log ε) 286 (4.25), 298 (4.23) nm; ECD (MeOH) λ_{max} ($\Delta\varepsilon$) 255 (−8.6), 282 (10.1), 292 (3.2), 302 (−0.3) nm; ^{1}H and ^{13}C NMR, see Tables 2 and 3; HRESIMS *m*/*z* 525.1707 $[M - H]^-$ (calcd for $C_{35}H_{25}O_5$, 525.1707); the MS/MS spectrum is deposited in the GNPS spectral library, https://gnps.ucsd.edu/ProteoSAFe/gnpslibraryspectrum.jsp?SpectrumID=CCMSLIB00004722192#%7B%7D.

*Selaginpulvilin T (**10**):* yellow oil; $[\alpha]_D^{20}$ +281 (*c* 1.0, MeOH); UV (MeOH) λ_{max} (log ε) 290 (4.29), 300 (4.28) nm; ECD (MeOH) λ_{max} ($\Delta\varepsilon$) 252 (1.3), 266 (4.3), 284 (−3.5), 292 (−2.1), 300 (−4.4) nm; ^{1}H and ^{13}C NMR, see Tables 2 and 3; HRESIMS *m*/*z* 539.1866 $[M - H]^-$ (calcd for $C_{36}H_{27}O_5$, 539.1863); the MS/MS spectrum is deposited in the GNPS spectral library, https://gnps.ucsd.edu/ProteoSAFe/gnpslibraryspectrum.jsp?SpectrumID=CCMSLIB00004722193#%7B%7D.

*Selaginellin (**11**):* yellow oil; UV (MeOH) λ_{max} (log ε) 206 (4.63), 267 (4.47), 301 (4.49), 434 (4.26) nm; ^{1}H and ^{13}C NMR, see Table S1 (Supporting Information); HRESIMS *m*/*z* 511.1544 $[M - H]^-$ (calcd for $C_{34}H_{23}O_5$, 511.1550); the MS/MS spectrum is deposited in the GNPS spectral library, https://gnps.ucsd.edu/ProteoSAFe/gnpslibraryspectrum.jsp?SpectrumID=CCMSLIB00004684197#%7B%7D.

*Selaginpulvilin A (**12**):* yellow oil; UV (MeOH) λ_{max} (log ε) 204 (4.60), 289 (4.34), 300 (4.35) nm; ^{1}H and ^{13}C NMR, see Table S2 (Supporting Information); HRESIMS *m*/*z* 511.1544 $[M - H]^-$ (calcd for $C_{34}H_{23}O_5$, 511.1550); the MS/MS spectrum is deposited in the GNPS spectral library, https://gnps.ucsd.edu/ProteoSAFe/gnpslibraryspectrum.jsp?SpectrumID=CCMSLIB00004722195#%7B%7D.

*Selaginpulvilin I (**13**):* yellow oil; UV (MeOH) λ_{max} (log ε) 285 (4.09) nm; ^{1}H and ^{13}C NMR, see Table S1; HRESIMS *m*/*z* 497.1402 $[M - H]^-$ (calcd for $C_{33}H_{21}O_5$, 497.1394); the MS/MS spectrum is deposited in the GNPS spectral library, https://gnps.ucsd.edu/ProteoSAFe/gnpslibraryspectrum.jsp?SpectrumID=CCMSLIB00004722197#%7B%7D.

*Selaginpulvilin K (**14**):* yellow oil; UV (MeOH) λ_{max} (log ε) 206 (4.67), 317 (4.37), 358 (4.28) nm; ^{1}H and ^{13}C NMR, see Table S2

DOI: 10.1021/acs.jnatprod.9b00049
J. Nat. Prod. 2019, 82, 1820–1830

(Supporting Information); HRESIMS m/z 537.1693 $[M - H]^-$ (calcd for $C_{36}H_{25}O_5$, 537.1707); the MS/MS spectrum is deposited in the GNPS spectral library, https://gnps.ucsd.edu/ProteoSAFe/gnpslibraryspectrum.jsp?SpectrumID=CCMSLIB00004722185#%7B%7D.

*Selaginpulvilin L (**15**):* yellow oil; UV (MeOH) λ_{max} (log ε) 207 (4.64), 286 (4.44), 299 (4.44) nm; ^1H and ^{13}C NMR, see Table S2 (Supporting Information); HRESIMS m/z 509.1743 $[M - H]^-$ (calcd for $C_{35}H_{25}O_4$, 509.1758); the MS/MS spectrum is deposited in the GNPS spectral library, https://gnps.ucsd.edu/ProteoSAFe/gnpslibraryspectrum.jsp?SpectrumID=CCMSLIB00004722198#%7B%7D.

Computation of ECD Data. For the analysis of the absolute configurations of C-1 in **1**, C-3 in **2**, and C-9 in **8**−**10**, conformational searches were performed using MMFF94s in Conflex 7 with an energy cutoff of 10.0 kcal/mol. Ground-state geometry optimization for the conformers was carried out by the def-SV(P) basis set for all atoms, B3LYP functional, and density functional theory (DFT) using TmoleX 3.4 and Turbomole (COSMOLogic GmbH, Leverkusen, Germany). After optimization, conformers with a Boltzmann distribution over 1% were chosen, and their ECD spectra were calculated with time-dependent DFT (TDDFT) at the B3LYP/def-SV(P) level. The individual ECD spectra were simulated by the SpecDis v.1.70.1 program by applying a Gaussian band shape with a sigma/gamma value of 0.16 eV for **1** and **2** and 0.30 eV for **8**−**10** for oscillator strengths and dipole-velocity rotational strengths, respectively. The predicted ECD spectrum was obtained using a Boltzmann population-weighted average and was plotted with Gnuplot v.5.2.

Enzymatic Assay of PDE4D2 Inhibition. The IMAP TR-FRET phosphodiesterase evaluation assay kit (Molecular Devices) was used to determine PDE4D2 inhibitory activity. PDE4D2 was obtained from BPS Bioscience (San Diego, CA, USA). The assays were conducted in black 96-well U-bottom plates. The manufacturer's instructions were followed during the assay. Briefly, PDE4D2 (5.0 pg/μL, 20 μL) was dispensed in IMAP assay buffer consisting of 10 mM Tris, pH 7.2, 10 mM $MgCl_2$, 0.05% NaN_3, 1 mM dithiothreitol, and 0.1% phosphate-free bovine serum albumin as the carrier. Plates were preincubated for 30 min at room temperature with test compounds or vehicle control (5 μL) before addition of 25 μL of substrate, which resulted in 200 nM FAM-cAMP in the reaction. The enzymatic reactions were allowed to proceed at room temperature for 60 min. The assay was terminated by adding 100 μL of IMAP-binding reagent Tb complex to each well. The plates were additionally incubated for 60 min at room temperature with gentle shaking. Finally the fluorescence intensity (FI) was measured by a SpectraMax M5 microplate reader using SoftMax Pro5 software (Molecular Devices, CA, USA). The FI was measured according to the manufacturer's recommendations using a SpectraMax M5 microplate reader. Curve fitting and IC_{50} values were determined with a four-parameter nonlinear regression using GraphPad Prism v7.0 (GraphPad Software Inc.). The experiments were performed for three independent replicates. Rolipram (Tokyo Chemical Industry, Tokyo, Japan) was used as a positive control.

Molecular Docking Study. The docking studies were performed with Accelrys Discovery Studio 2018 (BIOVIA, San Diego, CA, USA). The crystal structure of the catalytic domain of human PDE4D2 bound with selaginpulvlin K (RCSB Protein Data Bank code: 5WQA; https://www.rcsb.org) was applied for the docking studies. The crystallographic water molecules were removed, but those coordinated with the two metal ions Mg^{2+} and Zn^{2+} were retained in the structure. The CHARMM force field and the Momany-Rone partial charge method was used to add hydrogens and charges to the system. A neutral pH was hypothesized for the protonation states of all ionizable residues in the systems. The active site of PDE4D2 was defined using selaginpulvilin K as a reference compound; then other active compounds were docked into the site by using the CDOCKER protocol. The radius of the input site sphere was set as 10 Å from the center of the binding site, the pose cluster radius was set to 1.5, and 50 random conformations were generated for each ligand. Default values were used for other docking parameters. The interaction energies between the enzyme and inhibitors were calculated with implicit distance-dependent dielectrics using the Calculate Interaction Energy protocol.

■ ASSOCIATED CONTENT

Supporting Information

The Supporting Information is available free of charge on the ACS Publications website at DOI: 10.1021/acs.jnatprod.9b00049.

Detailed experimental procedures, raw NMR, HRMS, UV, and ECD spectra of compounds **1**−**15**, as well as detailed results of ECD, the calculation, PDE4 inhibitory assay, and molecular docking study (PDF)

■ AUTHOR INFORMATION

Corresponding Authors

*E-mail: kbkang@sookmyung.ac.kr. Tel: +82-2-2077-7103 (K. B. Kang).

*E-mail: jwkim@snu.ac.kr. Tel: +82-2-880-7853 (J. Kim).

ORCID

Sunmin Woo: 0000-0001-7561-2333

Kyo Bin Kang: 0000-0003-3290-1017

Jinwoong Kim: 0000-0001-9579-738X

Sang Hyun Sung: 0000-0002-0527-4815

Notes

The authors declare no competing financial interest.

§Deceased July 24, 2018.

■ ACKNOWLEDGMENTS

This research was supported by Sookmyung Women's University Specialization Program Funding (SP1-201809-6). We would like to thank Dr. Y.-J. Ko of the National Center for Interuniversity Research Facilities (NCIRF) at Seoul National University for her assistance with the NMR experiments.

■ REFERENCES

(1) Houslay, M. D.; Schafer, P.; Zhang, K. Y. J. *Drug Discovery Today* **2005**, *10*, 1503−1519.

(2) Lipworth, B. J. *Lancet* **2005**, *365*, 167−175.

(3) Pullamsetti, S. S.; Banat, G. A.; Schmall, A.; Szibor, M.; Pomagruk, D.; Hanze, J.; Kolosionek, E.; Wilhelm, J.; Braun, T.; Grimminger, F.; Seeger, W.; Schermuly, R. T.; Savai, R. *Oncogene* **2013**, *32*, 1121−1134.

(4) El-Elimat, T.; Figueroa, M.; Raja, H. A.; Graf, T. N.; Adcock, A. F.; Kroll, D. J.; Day, C. S.; Wani, M. C.; Pearce, C. J.; Oberlies, N. H. *J. Nat. Prod.* **2013**, *76*, 382−387.

(5) Lin, T. T.; Huang, Y. Y.; Tang, G. H.; Cheng, Z. B.; Liu, X.; Luo, H. B.; Yin, S. *J. Nat. Prod.* **2014**, *77*, 955−962.

(6) Zhang, L. P.; Liang, Y. M.; Wei, X. C.; Cheng, D. L. *J. Org. Chem.* **2007**, *72*, 3921−3924.

(7) Liu, X.; Luo, H. B.; Huang, Y. Y.; Bao, J. M.; Tang, G. H.; Chen, Y. Y.; Wang, J.; Yin, S. *Org. Lett.* **2014**, *16*, 282−285.

(8) Huang, Y. Y.; Liu, X.; Wu, D. Y.; Tang, G. H.; Lai, Z. W.; Zheng, X. H.; Yin, S.; Luo, H. B. *Biochem. Pharmacol.* **2017**, *130*, 51−59.

(9) Yao, W. N.; Huang, R. Z.; Hua, J.; Zhang, B.; Wang, C. G.; Liang, D.; Wang, H. S. *ACS Omega* **2017**, *2*, 2178−2183.

(10) Zhang, J. S.; Liu, X.; Weng, J.; Guo, Y. Q.; Li, Q. J.; Ahmed, A.; Tang, G. H.; Yin, S. *Org. Chem. Front.* **2017**, *4*, 170−177.

(11) Karmakar, R.; Lee, D. *Org. Lett.* **2016**, *18*, 6105−6107.

(12) Chinta, B. S.; Baire, B. *Org. Biomol. Chem.* **2017**, *15*, 5908−5911.

(13) Sowden, M. J.; Sherburn, M. S. *Org. Lett.* **2017**, *19*, 636−637.

(14) Henke, M. T.; Kelleher, N. L. *Nat. Prod. Rep.* **2016**, *33*, 942−950.

DOI: 10.1021/acs.jnatprod.9b00049
J. Nat. Prod. 2019, 82, 1820−1830

(15) Bouslimani, A.; Sanchez, L. M.; Garg, N.; Dorrestein, P. C. *Nat. Prod. Rep.* **2014**, *31*, 718−729.
(16) Wolfender, J. L.; Marti, G.; Thomas, A.; Bertrand, S. *J. Chromatogr. A* **2015**, *1382*, 136−164.
(17) Yao, H.; Chen, B.; Zhang, Y. Y.; Ou, H. G.; Li, Y. X.; Li, S. G.; Shi, P. Y.; Lin, X. H. *Molecules* **2017**, *22*, 325.
(18) Yobi, A.; Wone, B. W. M.; Xu, W. X.; Alexander, D. C.; Guo, L. N.; Ryals, J. A.; Oliver, M. J.; Cushman, J. C. *Mol. Plant* **2013**, *6*, 369−385.
(19) Watrous, J.; Roach, P.; Alexandrov, T.; Heath, B. S.; Yang, J. Y.; Kersten, R. D.; van der Voort, M.; Pogliano, K.; Gross, H.; Raaijmakers, J. M.; Moore, B. S.; Laskin, J.; Bandeira, N.; Dorrestein, P. C. *Proc. Natl. Acad. Sci. U. S. A.* **2012**, *109*, E1743−E1752.
(20) Yang, J. Y.; Sanchez, L. M.; Rath, C. M.; Liu, X. T.; Boudreau, P. D.; Bruns, N.; Glukhov, E.; Wodtke, A.; de Felicio, R.; Fenner, A.; Wong, W. R.; Linington, R. G.; Zhang, L. X.; Debonsi, H. M.; Gerwick, W. H.; Dorrestein, P. C. *J. Nat. Prod.* **2013**, *76*, 1686−1699.
(21) Bonneau, N.; Chen, G. M.; Lachkar, D.; Boufridi, A.; Gallard, J. F.; Retailleau, P.; Petek, S.; Debitus, C.; Evanno, L.; Beniddir, M. A.; Poupon, E. *Chem. - Eur. J.* **2017**, *23*, 14454−14461.
(22) Olivon, F.; Apel, C.; Retailleau, P.; Allard, P. M.; Wolfender, J. L.; Touboul, D.; Roussi, F.; Litaudon, M.; Desrat, S. *Org. Chem. Front.* **2018**, *5*, 2171−2178.
(23) Nguyen, D. D.; Wu, C. H.; Moree, W. J.; Lamsa, A.; Medema, M. H.; Zhao, X. L.; Gavilan, R. G.; Aparicio, M.; Atencio, L.; Jackson, C.; Ballesteros, J.; Sanchez, J.; Watrous, J. D.; Phelan, V. V.; van de Wiel, C.; Kersten, R. D.; Mehnaz, S.; De Mot, R.; Shank, E. A.; Charusanti, P.; Nagarajan, H.; Duggan, B. M.; Moore, B. S.; Bandeira, N.; Palsson, B. O.; Pogliano, K.; Gutierrez, M.; Dorrestein, P. C. *Proc. Natl. Acad. Sci. U. S. A.* **2013**, *110*, E2611−E2620.
(24) Wang, M. X.; Carver, J. J.; Phelan, V. V.; Sanchez, L. M.; Garg, N.; Peng, Y.; Nguyen, D. D.; Watrous, J.; Kapono, C. A.; Luzzatto-Knaan, T.; Porto, C.; Bouslimani, A.; Melnik, A. V.; Meehan, M. J.; Liu, W. T.; Criisemann, M.; Boudreau, P. D.; Esquenazi, E.; Sandoval-Calderon, M.; Kersten, R. D.; Pace, L. A.; Quinn, R. A.; Duncan, K. R.; Hsu, C. C.; Floros, D. J.; Gavilan, R. G.; Kleigrewe, K.; Northen, T.; Dutton, R. J.; Parrot, D.; Carlson, E. E.; Aigle, B.; Michelsen, C. F.; Jelsbak, L.; Sohlenkamp, C.; Pevzner, P.; Edlund, A.; McLean, J.; Piel, J.; Murphy, B. T.; Gerwick, L.; Liaw, C. C.; Yang, Y. L.; Humpf, H. U.; Maansson, M.; Keyzers, R. A.; Sims, A. C.; Johnson, A. R.; Sidebottom, A. M.; Sedio, B. E.; Klitgaard, A.; Larson, C. B.; Boya, C. A.; Torres-Mendoza, D.; Gonzalez, D. J.; Silva, D. B.; Marques, L. M.; Demarque, D. P.; Pociute, E.; O'Neill, E. C.; Briand, E.; Helfrich, E. J. N.; Granatosky, E. A.; Glukhov, E.; Ryffel, F.; Houson, H.; Mohimani, H.; Kharbush, J. J.; Zeng, Y.; Vorholt, J. A.; Kurita, K. L.; Charusanti, P.; McPhail, K. L.; Nielsen, K. F.; Vuong, L.; Elfeki, M.; Traxler, M. F.; Engene, N.; Koyama, N.; Vining, O. B.; Baric, R.; Silva, R. R.; Mascuch, S. J.; Tomasi, S.; Jenkins, S.; Macherla, V.; Hoffman, T.; Agarwal, V.; Williams, P. G.; Dai, J. Q.; Neupane, R.; Gurr, J.; Rodriguez, A. M. C.; Lamsa, A.; Zhang, C.; Dorrestein, K.; Duggan, B. M.; Almaliti, J.; Allard, P. M.; Phapale, P.; Nothias, L. F.; Alexandrovr, T.; Litaudon, M.; Wolfender, J. L.; Kyle, J. E.; Metz, T. O.; Peryea, T.; Nguyen, D. T.; VanLeer, D.; Shinn, P.; Jadhav, A.; Muller, R.; Waters, K. M.; Shi, W. Y.; Liu, X. T.; Zhang, L. X.; Knight, R.; Jensen, P. R.; Palsson, B. O.; Pogliano, K.; Linington, R. G.; Gutierrez, M.; Lopes, N. P.; Gerwick, W. H.; Moore, B. S.; Dorrestein, P. C.; Bandeira, N. *Nat. Biotechnol.* **2016**, *34*, 828−837.
(25) Ruttkies, C.; Schymanski, E. L.; Wolf, S.; Hollender, J.; Neumann, S. *J. Cheminformatics* **2016**, *8*, 3.
(26) da Silva, R. R.; Wang, M. X.; Nothias, L. F.; van der Hooft, J. J. J.; Caraballo-Rodriguez, A. M.; Fox, E.; Balunas, M. J.; Klassen, J. L.; Lopes, N. P.; Dorrestein, P. C. *PLoS Comput. Biol.* **2018**, *14*, No. e1006089.
(27) Kang, K. B.; Park, E. J.; da Siva, R. R.; Kim, H. W.; Dorrestein, P. C.; Sung, S. H. *J. Nat. Prod.* **2018**, *81*, 1819−1828.
(28) Zhu, Q.-F.; Bao, Y.; Zhang, Z.-J.; Su, J.; Shao, L.-D.; Zhao, Q.-S. *R. Soc. Open Sci.* **2017**, *4*, 170352.
(29) Bender, A. T.; Beavo, J. A. *Pharmacol. Rev.* **2006**, *58*, 488−520.
(30) Wu, G. S.; Robertson, D. H.; Brooks, C. L.; Vieth, M. *J. Comput. Chem.* **2003**, *24*, 1549−1562.
(31) Card, G. L.; England, B. P.; Suzuki, Y.; Fong, D.; Powell, B.; Lee, B.; Luu, C.; Tabrizizad, M.; Gillette, S.; Ibrahim, P. N.; Artis, D. R.; Bollag, G.; Milburn, M. V.; Kim, S. H.; Schlessinger, J.; Zhang, K. Y. J. *Structure* **2004**, *12*, 2233−2247.
(32) Ke, H. M.; Wang, H. C. *Curr. Top. Med. Chem.* **2007**, *7*, 391−403.
(33) Nothias, L. F.; Nothias-Esposito, M.; da Silva, R.; Wang, M. X.; Protsyuk, I.; Zhang, Z.; Sarvepalli, A.; Leyssen, P.; Touboul, D.; Costa, J.; Paolini, J.; Alexandrov, T.; Litaudon, M.; Dorrestein, P. C. *J. Nat. Prod.* **2018**, *81*, 758−767.
(34) Philippus, A. C.; Zatelli, G. A.; Wanke, T.; Barros, M. G. D.; Kami, S. A.; Lhullier, C.; Armstrong, L.; Sandjo, L. P.; Falkenberg, M. *RSC Adv.* **2018**, *8*, 29654−29661.
(35) Chambers, M. C.; Maclean, B.; Burke, R.; Amodei, D.; Ruderman, D. L.; Neumann, S.; Gatto, L.; Fischer, B.; Pratt, B.; Egertson, J.; Hoff, K.; Kessner, D.; Tasman, N.; Shulman, N.; Frewen, B.; Baker, T. A.; Brusniak, M. Y.; Paulse, C.; Creasy, D.; Flashner, L.; Kani, K.; Moulding, C.; Seymour, S. L.; Nuwaysir, L. M.; Lefebvre, B.; Kuhlmann, F.; Roark, J.; Rainer, P.; Detlev, S.; Hemenway, T.; Huhmer, A.; Langridge, J.; Connolly, B.; Chadick, T.; Holly, K.; Eckels, J.; Deutsch, E. W.; Moritz, R. L.; Katz, J. E.; Agus, D. B.; MacCoss, M.; Tabb, D. L.; Mallick, P. *Nat. Biotechnol.* **2012**, *30*, 918−920.
(36) Frank, A. M.; Bandeira, N.; Shen, Z.; Tanner, S.; Briggs, S. P.; Smith, R. D.; Pevzner, P. A. *J. Proteome. Res.* **2008**, *7*, 113−122.

DOI: 10.1021/acs.jnatprod.9b00049
J. Nat. Prod. 2019, 82, 1820−1830